Pharmaceutical Research, Vol. 24, No. 6, June 2007 (© 2007)
DOI: 10.1007/s11095-007-9250-3

Expert Review

Promise and Progress for Functional and Molecular Imaging of Response to Targeted Therapies

Renu M. Stephen[1,2] and Robert J. Gillies[1]

Received December 1, 2006; accepted January 23, 2007; published online March 24, 2007

Abstract. Biomarkers to predict or monitor therapy response are becoming essential components of drug developer's armamentaria. Molecular and functional imaging has particular promise as a biomarker for anticancer therapies because it is non-invasive, can be used longitudinally and provides information on the whole patient or tumor. Despite this promise, molecular or functional imaging endpoints are not routinely incorporated into clinical trial design. As the costs of clinical trials and drug development become prohibitively more expensive, the need for improved biomarkers has become imperative and thus, the relatively high cost of imaging is justified. Imaging endpoints, such as Diffusion-Weighted MRI, DCE-MRI and FDG-PET have the potential to make drug development more efficient at all phases, from discovery screening with *in vivo* pharmacodynamics in animal models through the phase III enrichment of the patient population for potential responders. This review focuses on the progress of imaging responses to new classes of anti-cancer therapies targeted against PI3 kinase/AKT, HIF-1α and VEGF. The ultimate promise of molecular and functional imaging is to theragnostically predict response prior to commencement of targeted therapy.

KEY WORDS: DCE-MRI; Diffusion-Weighted MRI; FDG-PET; HIF-1α; imaging biomarkers; PI3K-AKT; targeted therapies; VEGF.

INTRODUCTION

Over the last decade, the changes in diagnostic imaging have been nothing short of revolutionary. What used to be a discipline focused on anatomy has been transformed to one that can measure tissue function as well as expression of specific molecules. This has occurred primarily through advances in Magnetic Resonance Imaging (MRI) and Positron Emission Tomography (PET) with somewhat lesser contributions from other imaging modalities, such as Single Photon Emitted Computed Tomography (SPECT), ultrasound and X-ray CT.

Therapeutic clinical trials are an important venue that can be significantly impacted by the application of these newer molecular and functional imaging modalities. As these are applied in combination with molecular biomarkers, they will guide the practice of oncology towards individualized therapy. These imaging endpoints also have the potential to make drug development and clinical trials more efficient. Despite the promise and progress in molecular and functional imaging, these approaches have yet to be incorporated into the mainstream of clinical trial design. As of 2004, molecular or functional imaging was only being used in approximately 10% of phase I/II anti-cancer therapy trials while toxicity and pharmacokinetics have continued to remain as the familiar gauge in determining recommended dose (1).

[1] Arizona Cancer Center, University of Arizona, 1515 N. Campbell P.O. box: 245024 Tucson, Arizona 85724, USA.
[2] To whom correspondence should be addressed. (e-mail: rms3@email.arizona.edu)

MOLECULAR AND FUNCTIONAL IMAGING OF CANCER

Molecular imaging generally uses contrast agents or tracers that interact with tissue in a molecularly specific fashion, whereas functional imaging can use endogenous or exogenous contrast to provide information on tissue phenotype or behavior. Because the demarcation between these approaches is fuzzy, we prefer the single moniker, Molecular and Functional Imaging. Because of its promise, substantial resources have been put into molecular and functional imaging of cancer over the last decade with the expectation for exciting new research opportunities and clinical translation (http://imaging.cancer.gov/). Molecular and functional imaging involves non-invasive measures that have distinct advantages over traditional tissue sampling. Although tissue biopsies provide important information regarding molecular pathology, the sampled tissue may not adequately represent the heterogeneity of tumors and furthermore cannot be sampled longitudinally. Non-invasive imaging can allow for repeated non-destructive assessment of molecular phenotype and provide spatial and temporal information regarding target organs, tumors or the entire body (2). Hence, molecular and functional imaging can be used to complement tissues biopsies and histopathological methods.

Another limitation of traditional monitors of anti-cancer treatments is the lack of longitudinal information obtained regarding metabolism and pathophysiology of individual tumors during therapy. Such information would allow for the early detection and monitoring of molecular or physio-

Table I. MR Imaging Biomarkers for Anti–cancer Therapies

Imaging Endpoint	What it Measures and How it is Used	Refs.
Low MW DCE-MRI	Tumor blood flow, extraction rate (K^{trans}), and interstitial volume. K^{trans} is reduced with anti-angiogenics but has high variance.	(43–48)
High MW DCE–MRI	Vessel permeability, vascular volume fraction. Low Variance. Sensitive to many drugs pre-clinically. Experimental in humans.	(49,50)
Diffusion-Weighted MRI	Sensitive to the intra- and extracellular volume ratio. Changes in response to cytotoxic therapies.	(5,8)
FDG-PET	Uptake and trapping of glucose analog. Metastatic cancers have elevated glycolysis and FDG trapping.	(51,52)

logical alterations prior to changes in tumor size and could guide the development of new targeted therapies. In practice, a relatively limited set of imaging endpoints have been applied to quantitatively monitor patient response to targeted anti-cancer therapies. These include Diffusion-Weighted (DW) MRI, Dynamic Contrast Enhanced (DCE) MRI, Magnetic Resonance Spectroscopy (MRS) and PET studies using fluorodeoxyglucose and other tracers (3–6).

MAGNETIC RESONANCE IMAGING

In Magnetic Resonance Imaging, patients are placed in a strong magnetic field gradient that causes MR-active nuclei to resonate at field-dependent frequencies. These are interrogated by radiofrequency pulses to generate images. In MRI, the observed signal is typically from the hydrogen nuclei (protons) on water and fat molecules because (a) hydrogen is the most sensitive biologically relevant NMR-active atom and (b) it is highly abundant *in vivo*. Water hydrogens are $\approx$ 110 Molar and the -CH_2 methylene protons on highly mobile lipids are also abundant enough to be visible by MRI. Depending on need, either the lipid or the water signal can be "suppressed," so that only the signals from other classes of protons are visible. The images acquired provide a wealth of information regarding tumor metabolism, vascularization and pathophysiology (3,7). Moreover, non-destructive data obtained from cell or animal models can be readily translated over into the clinical setting. A large number of imaging approaches are currently being used with some of these being well-developed and applicable in the clinic today (Table I). For the purpose of this review, we will focus on Diffusion-Weighted and Dynamic Contrast Enhanced MRI as the major MRI endpoints. These will be compared and contrasted to FDG-PET scanning.

DIFFUSION-WEIGHTED MRI

Diffusion-Weighted MRI measures the random microscopic motion of water protons by measuring signal decay between two balanced pulses of magnetic field gradients. If water is stationary, these pulses cancel each other out and 100% of the signal is obtained. If water is in motion, the pulses have unequal effects and signal is lost according to the relationship, $S=S_0\, e^{-bD}$, where 'D' is the (apparent) diffusion coefficient and 'b' is a factor that includes the gradient pulses strength, G, and the time between gradients pulses, Δ. The higher the b-factor, the greater the diffusion weighting. In tissues, the free diffusion of water is restricted by membrane and protein barriers (3,8). Thus, water diffusion is lower in tissues with high cell density than it is in pure water or tissues with edema or low cellularity. In quantitative diffusion MRI, a series of images are obtained at different b-values, and the data are fit to the above relationship on a pixel-by-pixel basis to generate maps of the apparent diffusion coefficient (ADC). Thus ADC maps are able to detect microstructural changes in cell membrane integrity and alterations in intra- *vs.* extracellular compartments prior to changes in tumor volume that occur with therapy (8). Diffusion-Weighted MRI has been used clinically to measure therapy response in brain tumors (9–14), GI cancers (15), osteosarcomas (16) and metastatic breast cancer (17). These have generally shown that an increase in ADC is observed early on (1–2 weeks) following commencement of successful therapy. Notably, some studies have indicated that a low pre-therapy ADC can predict response (18,19). As a low ADC is observed in tissues with high cell density, these results would suggest that tumors with higher cell density are more likely to respond to therapy.

In pre-clinical animal models, increases in ADC have been observed in cancers including fibrosarcomas, breast and prostate in response to a wide variety of non-targeted therapies, such as cisplatin, BCNU, taxanes and fluorouracil (8). In RIF-1 tumors, treatment with cyclophosphamide resulted in a 67% tumor cell kill which in turn lead to an increase in ADC values within 2 days that was seen in changes in tumor volume (20). In breast and prostate cancer xenografts, an increase in the ADC is a predictor of response to taxanes or combretastatin, which are targeted against tubulins (21–24). A number of groups are beginning to investigate the application of diffusion-weighted MRI to monitor response to therapies targeted against specific signal transduction pathways. In our group, Jordan *et al.* (5) demonstrated a significant increase in ADC at 24 h and 36 h following treatment with the HIF-1α inhibitor, PX-478, before returning to baseline (Fig. 1). Chinnaiyan *et al.* (25) demonstrated that ionizing radiation sensitized breast cancer cells to tumor necrosis factor-related apoptosis-inducing ligand (TRAIL) by the upregulation of a TRAIL receptor. DW-MRI was used here to identify changes in cellularity due to the combination of radiation and TRAIL and to assess its therapeutic efficacy. Rustamzadeh *et al.* (26) examined the efficacy of a human interleukin-13 and diphtheria toxin fusion protein to target human glioblastoma cell lines in a murine intracranial model using DW-MRI. DW-MRI was able to assess cellular toxicity and detect reductions in tumor volume as

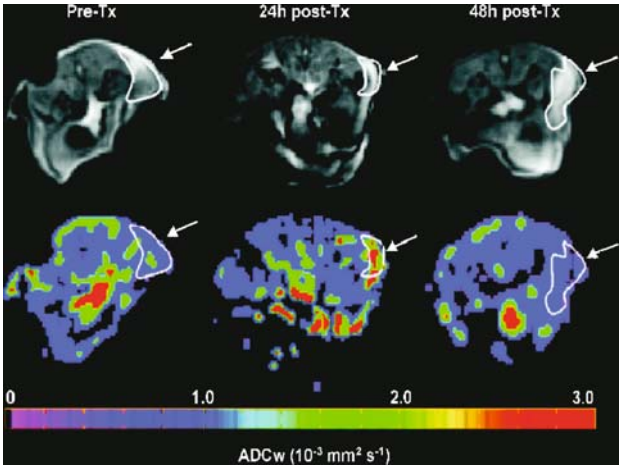

Fig. 1. DW images at a b value of 25 (*top row*) and corresponding diffusion maps (*bottom row*) of an HT-29 tumor-bearing mouse at 0, 24, and 48 h following PX-478 injection. Decrease in tumor cellularity was noted at 24 and 36 h following treatment as indicated with an increase in ADCw values. Each image represents an axial slice of the mouse with the tumor area *encircled and indicated by an arrow*.

well as support the efficacy of this fusion protein in an intracranial model.

DYNAMIC CONTRAST ENHANCED MRI

Dynamic Contrast Enhanced MRI follows the time course of signal enhancement following a bolus injection of a contrast agent into the vasculature. DCE-MRI is non-invasive and is sensitive to tumor perfusion parameters of vasculature volume, vascular permeability and flow. Serial images are acquired before, during and after injection of contrast agents which are typically chelates of lanthanides, most commonly gadolinium (Gd) (5,27). Transition element metals such as manganese (28) and iron (29) have also been used as contrast agents.

The intensity of enhancement as the contrast agent washes in and out of the intravascular and extravascular spaces provide information regarding the vasculature and permeability and can be used to discriminate between benign and malignant tissues. Typically more aggressive tumors are characterized by a rapid enhancement followed by a subsequently rapid wash-out period (30,31). Small molecular weight contrast agents such as Gd-DTPA are currently being used extensively in the clinics. However, these small molecular weight agents are not ideal to distinguish changes in perfusion that occur with therapy, because their wash-in and wash-out kinetics are so rapid, which necessitates rapid image acquisition and consequent reduction in image resolution. Furthermore, the vascular permeability is generally high, and thus these small agents will continue to extravasate even after therapy (3). Larger molecular weight molecules such as Gd-DTPA conjugated to Bovine Serum Albumin (Gd-DTPA-BSA), Gadomer-17 (Schering) or P-792 (Guerbet) may be more attractive as they can discriminate between more or less leaky microvessels. Hence, they may provide a fuller picture of the vasculature and permeability networks due to their longer intravascular retention times (7). Jordan *et al.* (5) demonstrated a dramatic reduction in tumor blood vessel permeability using Gd-BSA within 2 h following treatment with PX-478 (Fig. 2). DCE-MRI has enormous potential to measure tumor response to anti-cancer therapies that affect angiogenesis or perfusion.

^{18}F-FLUORODEOXYGLUCOSE POSITRON EMISSION TOMOGRAPHY AND GLUCOSE UPTAKE

Positron Emission Tomography is a radiological technique that involves the acquisition of physiologic images based on the detection of radiation from emitting positrons. In general, radioactive nuclei are introduced to the body as labels on tracer molecules. Frequently used tracers for PET imaging include ^{15}O, ^{13}N, ^{11}C and ^{18}F. These radioactive nuclei emit positively

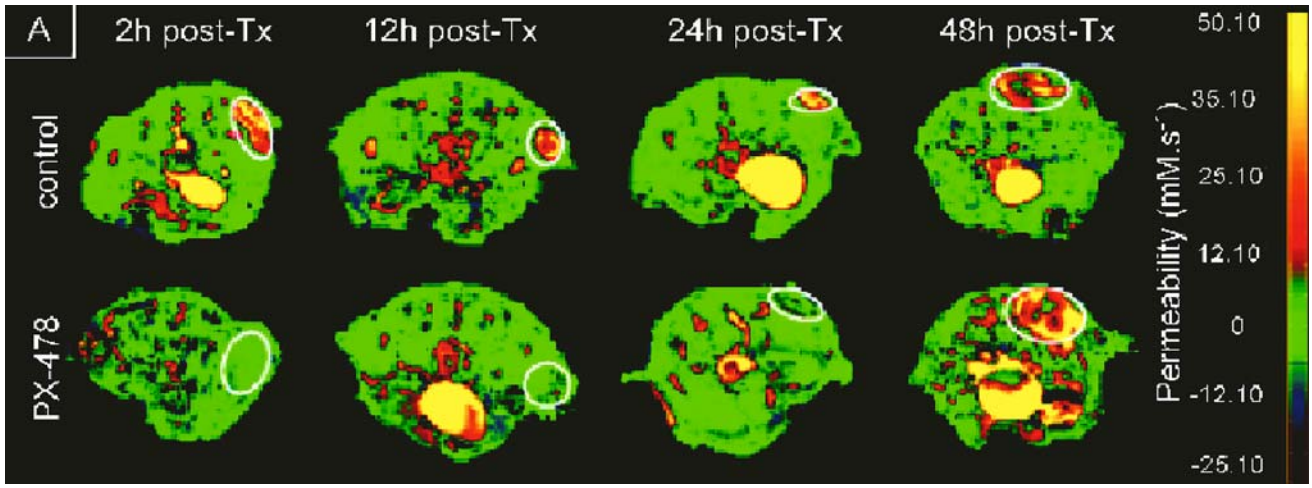

Fig. 2. Permeability maps of tumors at 2, 12, 24, and 48 h following injection of vehicle (control) or PX-478 (drug) injection. Each image represents an axial slice of the mouse with the *tumor area encircled*. A substantial decrease in tumor permeability was observed as early as 2 h following treatment and continuing until 24 h, in comparison to controls.

Fig. 3. Position Emission Tomography imaging with ^{18}fluorodeoxyglucose of a patient with lymphoma. The mediastinal nodes (*purple arrow*) and supraclavicular nodes (*green arrows*) show high uptake of ^{18}fluorodeoxyglucose (FDG), showing that tumors in these nodes have high levels of FDG uptake. The bladder (*yellow arrow*) also has high activity because of excretion of the radionuclide.

charged positrons that annihilate with an electron in tissue to produce a reaction resulting in the release of two 512 keV gamma rays that are 180° apart. These gamma rays easily pass through tissues where they are captured by a ring of detectors that detect simultaneously occurring events. Coincidence detection is used to pinpoint the source by a straight line along which the event took place (32).

PET has drawn much attention particularly in the early detection and staging of cancer and in evaluating response to therapy. Another powerful aspect of PET imaging is its ability to generate whole-body images, which is ideal for examining metastatic disease. Metastatic cancers invariably have increased glucose metabolism and, hence, they rapidly take up and phosphorylate (trap) ^{18}Fluorodeoxyglucose (^{18}FDG). ^{18}FDG is used in more than 90% of all cancer-related PET scans (33). It is transported via the glucose transporter GLUT-1 (or GLUT-3) into the cell where it is phosphorylated by hexokinase (II) and hence, trapped. The rate of ^{18}FDG trapping is used as a marker of malignancy as more aggressive tumors take up glucose more avidly due to an upregulation of glucose transporters (GLUT 1 and 3) and hexokinases (I and II) (34,35). Tissues with increased glucose uptake have positive ^{18}FDG PET scans with specificity and sensitivity around 90% (36); Fig. 3). Numerous studies involving ^{18}FDG PET have also correlated poor prognosis and tumor aggressiveness with increased ^{18}FDG uptake (37,38). In addition to staging tumors, ^{18}FDG PET has proven to be efficacious in evaluating response to therapy in a variety of cancers including breast (39,40), lung (41) and colorectal (42) by monitoring glucose uptake following treatment. The clinical relevance here is early identification of response to therapy and as a result more individualized and effective treatment to patients.

THE NEED FOR BIOMARKERS IN DRUG DEVELOPMENT

The achievements in molecular oncology in the past decade have been remarkable. With these, the hope of improved clinical outcomes has risen. Despite this potential, there has been a decrease in the number of new drugs to reach the market, and in recent years a decrease in the number of new drug applications (53). A possible reason for this is costs as the development of new therapies is becoming prohibitively expensive. It has been estimated that $1.6 billion in research and development is spent (equally split between government and PhRMA) for each new approved drug (54). This cost is approximately 50% higher than just 10 years ago and this increase has primarily occurred in the cost of conducting clinical trials where sensitivity, stability and reproducibility are all rigorously tested. These costs are being transferred over to the patients as the average cost of newly targeted cancer treatments has increased from about $20,000 / patient / year to roughly $100,000 / patient / year (55,56). Hence, there is a significant interest and effort towards reducing the costs of clinical trials by making them more efficient. Biomarkers are a quantifiable process that respond to, or predict, drug action. It is hypothesized that appropriate biomarkers can improve efficiency, and hence reduce costs, during all phases of drug development.

The advantage of using biomarkers is proof-of-principle studies that can be done for novel targeted therapies early on in the developmental process. This will allow for a more streamlined approach in identifying efficacious targets that will improve clinical outcome. Identifying these targets has multifaceted benefits to the patient and to investors. To the patient the greatest advantage would be early detection and more individualized treatment based on their tumor characteristics, as the heterogeneity of tumors are far more complex than originally thought. A perfect example is the recent identification of a large number of previously uncharacterized candidate cancer (CAN) genes in breast and colorectal cancers by Velculescu *et al.* (57) at Johns Hopkins. These genes, which affect a wide variety of cellular functions, provide potentially new therapeutic targets and reinforces the need for individualized treatment based on tumor type and individual characteristics and less to generic treatments. Patient stratification based on targeted therapies can guide treatment decisions. An example is herceptin, a drug given to breast cancer patients who overexpress the Her-2/neu receptor.

Identifying therapies for individual patients can prevent adverse drug reactions and increase survival by avoiding ineffective treatments. To PhRMA, identifying sub-populations

that will respond to therapy will help in the development of more targeted drugs therapies at reduced costs. In choosing appropriate markers, one must consider not only its sensitivity and specificity but also the feasibility and ease with which they can be translated over to the clinical setting. Non-invasive molecular imaging has enormous potential to improve clinical trial efficiency and aide in the development of targeted therapies.

IMAGING BIOMARKERS

An important hypothesis that remains to be proved is that molecular and functional imaging can make clinical trials more efficient. Imaging can potentially impact all areas of drug development (Table II). In drug discovery, *in vivo* imaging can be used to measure pharmacodynamics in high cell content and animal-based drug screens. In phase I clinical trials, biomarkers can be used to monitor pharmacodynamics by determining dose response of imaging endpoints. In phase II, changes in imaging parameters can be used to monitor therapy response and, in some cases, predict clinical outcome. During phase II, images are obtained pre-therapy and these can be analyzed retrospectively to determine if a functional imaging biomarker was predictive of sensitivity or response. If so, phase III could incorporate the use of biomarkers as an inclusion criteria, which would have a great impact on clinical trial efficiency. Phase IV and clinical practice would then use these biomarkers as an indication for use of the drug. Moreover, the utilization of imaging biomarkers to stratify patients based on therapy response can reduce the numbers of patients required for clinical trials by up to 16-fold (58,59). Streamlining clinical trials to be even slightly more efficient can easily translate to millions of dollars in savings and a decrease in the time for a drug to reach the market (60).

Molecular and Functional imaging biomarkers have generated interest because they are able to identify the location of disease as well as be used thera(g)nostically to assess response, diagnose and segment patients based on response, and elucidate the mechanisms of therapy response and resistance. An underlying hypothesis in our laboratory is that pre-clinical imaging in appropriate animal models can be predictive of responses in humans. If true, this would be advantageous in that many more imaging endpoints can be tested in animals in less time and for less money, than in humans. Furthermore, the issue of which imaging biomarker is appropriate and at what time post-therapy could be better elucidated early on. Testing this hypothesis depends critically on having a substantial base of animal data for drug-tumor combinations. This will also depend on having a clinical trial environment receptive to the use of these data.

Table II. Imaging Applications

Stages of Imaging	
Discovery	High content screening *in vitro* and *in vivo*
Phase I	Noninvasive measure of *in vivo* pharmacodynamics and pharmacokinetics
Phase II	Quantitative biomarker of therapy response
Phase III	Predictive biomarker of response for patient segmentation in trials
Clinical Practice	If approved, imaging results can be used as indicator

The incorporation of imaging endpoints into clinical trials is being supported by initiatives from the Food and Drug Administration (FDA), the National Institutes of Health (NIH), the Radiological Society of North America (RSNA), Pharmaceutical Research and Manufacturers of America (PhRMA), the American College of Radiology (ACR), the Society of Nuclear Medicine (SNM) and the Association of American Cancer Institutes (AACI). These are being organized into a network wherein the RSNA and ACR are spearheading the adoption of uniform protocols for imaging in clinical trials, UPICT (http://upict.acr.org/). PhRMA is working on an agreement for data sharing amongst its members, the FDA and the NIH, as part of their Critical Path Initiative have developed (and are continuing to develop) guidelines for the inclusion of imaging data into drug approval (http://www.fda.gov/cder/regulatory/medImaging/default.htm). Additionally, the NIH in partnership with the AACI has established a national consortium of Imaging Response Assessment Teams (http://www.aaci-cancer.org/).

TARGETED THERAPIES

The utilization of molecular imaging to identify response to therapy relies on having validated cancer drug targets. Ideal cancer targets are those that are specific to molecules involved in proliferation and apoptosis, cell invasion and metastatic spread, and angiogenesis but yet are not toxic to normal cells. Over the past five years, the number of novel targets has risen as signaling pathways involved in cancer progression have become better elucidated (61,62). For the purposes of this review, we will focus on three anti-cancer therapy targets to represent targets where there has been no imaging (PI3K-AKT); a little imaging (HIF1-α) and extensive imaging (VEGF/VEGF-R).

PHOSPHATIDYLINOSITOL-3-KINASE (PI3K)-AKT

Phosphatidylinositol-3-kinase is a key regulator of fundamental cellular functions including transcription, translation, proliferation, growth and survival (63,64); Fig. 4). Constitutive activation of the PI3K-AKT signaling pathway has been associated with the development of cancer and drug resistance (65–67) as well as diabetes and autoimmunity (68,69). PI3K, a heterodimeric lipid kinase composed of regulatory and catalytic subunits, is responsible for the phosphorylation of the 3′-OH group of the inositol ring to produce phosphatidylinositol-3,4,5-triphosphate (PIP3). The PTEN (phosphatase and tensin homologue deleted on chromosome 10) tumor suppressor is a PIP3 phosphatase that acts to convert PIP3 back to PIP2. It is inactivated through deletion or mutation in many cancers resulting in constitutively high levels of PIP3 (64). PIP3 acts as a scaffold for plekstrin-homology (PH) domain containing proteins such as AKT. AKT is a 57 kD member of the Ser/Thr kinase family that acts downstream of PI3K to regulate processes involved in cell survival and proliferation (70). There are three mammalian AKT genes, AKT1(PKBα), AKT2(PKBβ),

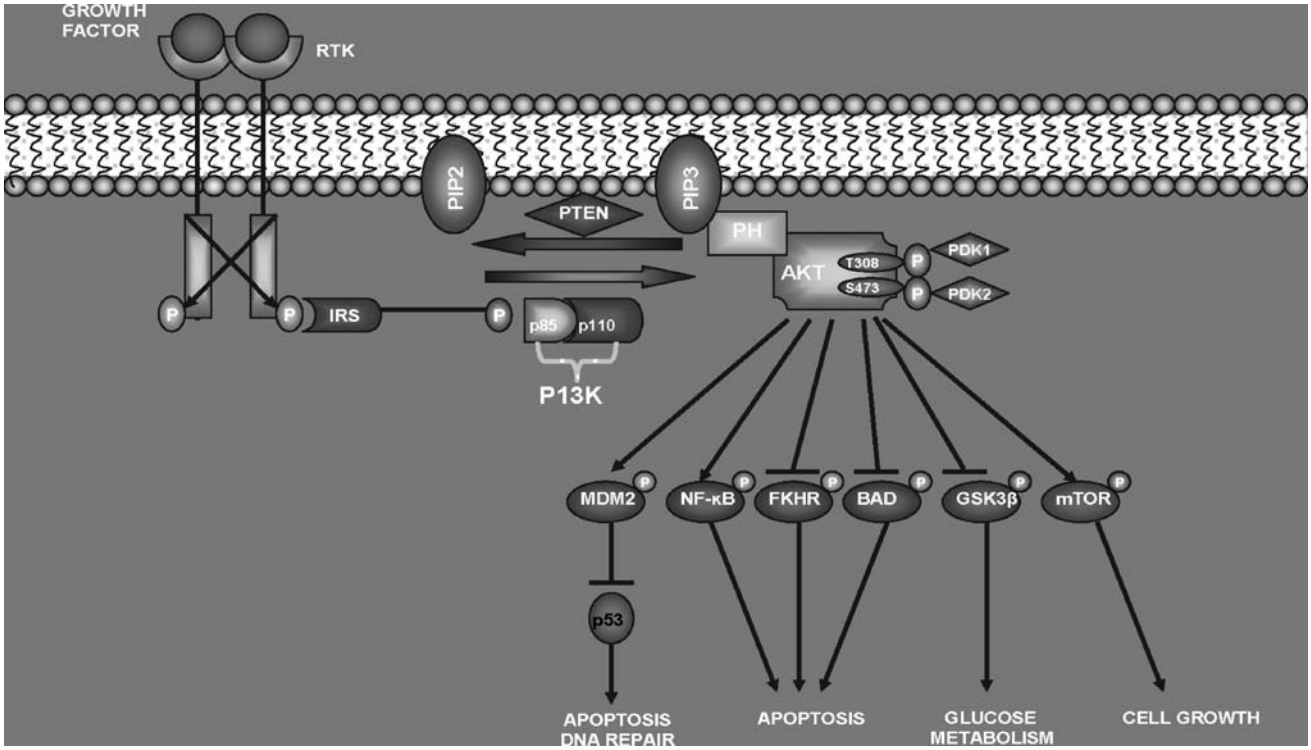

Fig. 4. PI3K-AKT pathway and the downstream effects of phosphorylated AKT.

and AKT3(PKBγ) that are widely expressed in various tissues (67). Following binding of the PH domain to PIP3, AKT is translocated to the plasma membrane where it is activated via phosphorylation on Thr^{308} and Ser^{473} by membrane kinases, such as phosphoinositide-dependent kinase 1 and 2 , PDK1 and PDK2 (67,71–73). Activated p-AKT phosphorylates a number of targets involved in cell growth, metabolism and survival.

Targeted Therapy and Functional and Molecular Imaging

PI3K inhibitors are a major target in inhibiting AKT activation and tumor progression. Wortmannin, LY294002 and PX-866 are anti-cancer drugs used in inhibiting the PI3K-AKT pathway. Wortmannin and LY294002 are potent inhibitors of PI3K and have been shown to sensitize tumor cells to other targeted therapies including chemo- and

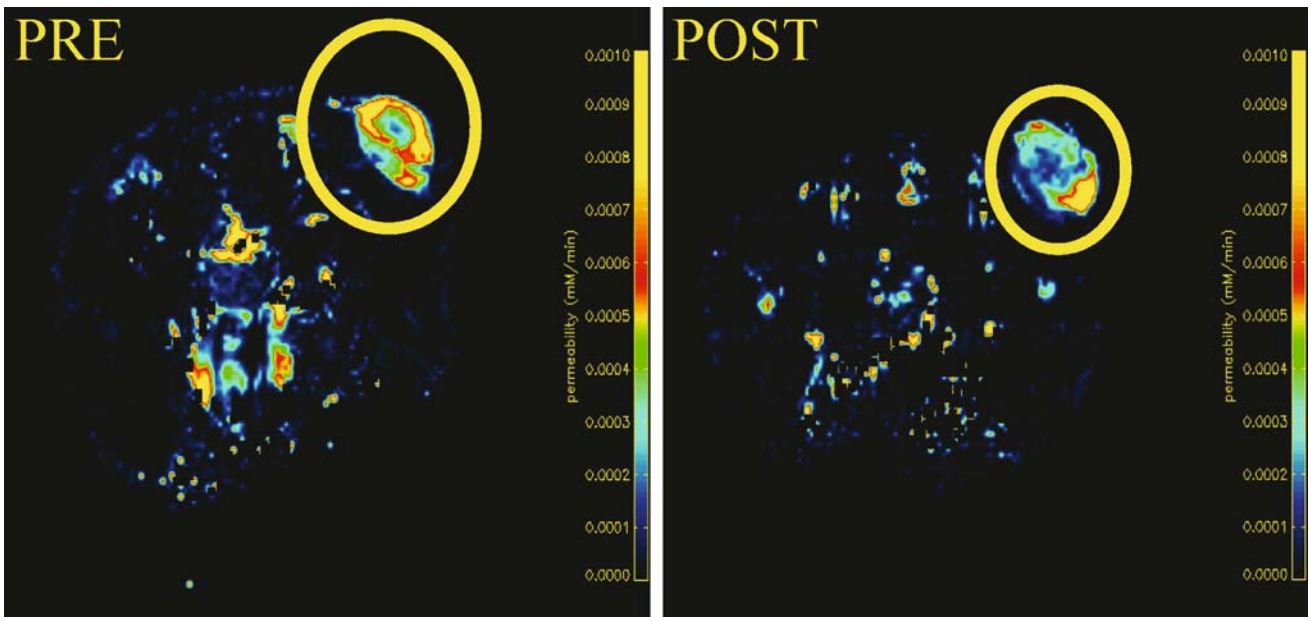

Fig. 5. Permeability maps of HT-29 tumors following injection of PX-866. A decrease in tumor permeability was observed at 48 h following therapy. Each image represents an axial slice of the mouse with the *tumor area encircled*.

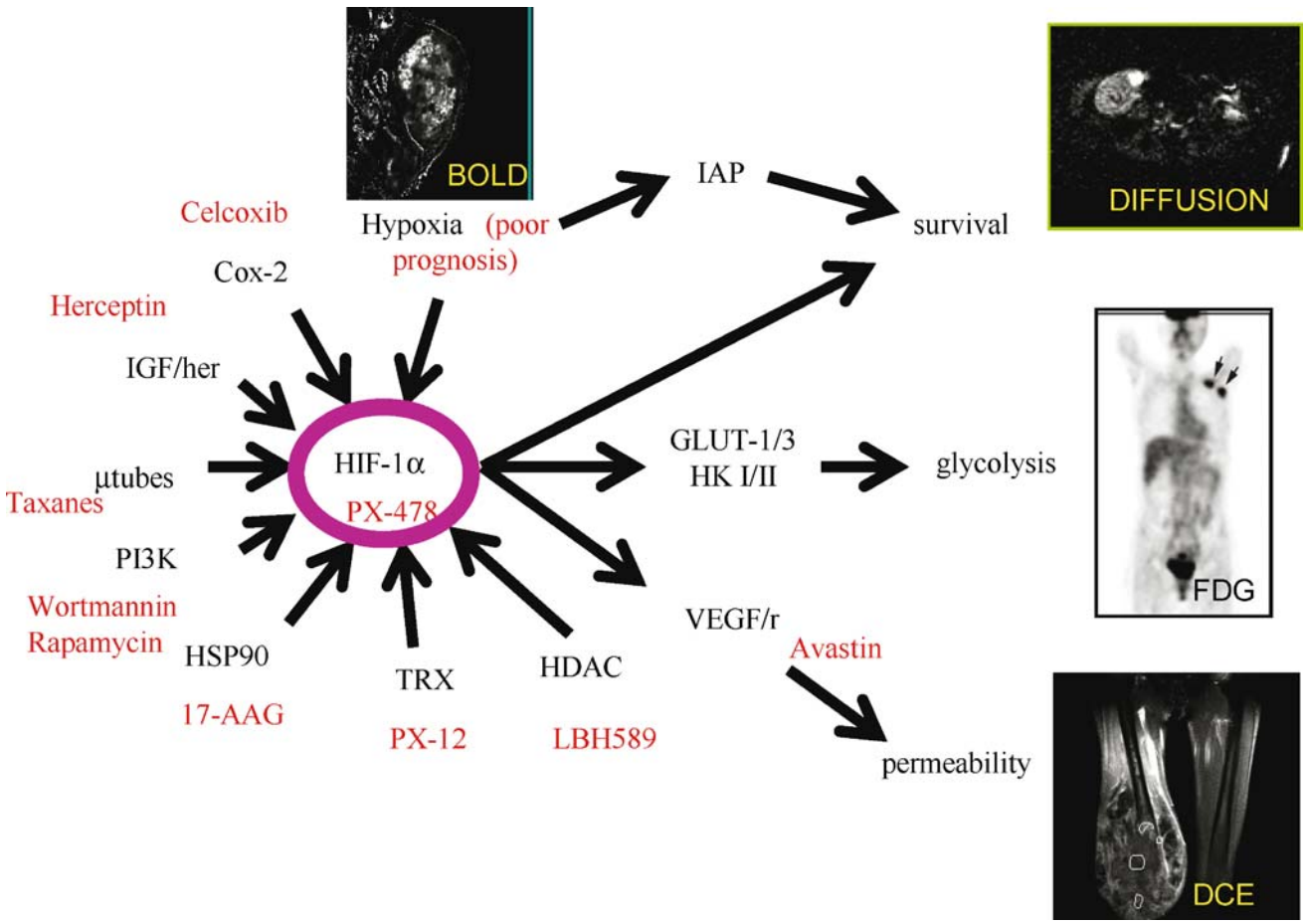

Fig. 6. HIF-1α is stabilized by a number of factors, including (CCW from top) hypoxia, cyclooxygenase-2, insulin-like growth factor-2/EGF receptor, microtubule stabilization, PI3 kinase/Akt, heat shock protein-90, thioredoxin and histone deacetylase. All of these are targets for therapies, *indicated in red*. HIF-1α is a survival factor and this, combined with hypoxic induction of xIAP (inhibitor of apoptosis) will lead to increased survival, measurable with diffusion MRI. HIF-1α induction of glycolysis via glucose transport and phosphorylation is measurable with FDG-PET. HIF-1α induction of angiogenesis via VEGF and its receptor are measurable via dynamic contrast enhanced MRI. Thus the actions of these drugs is potentially measurable by these relatively distal imaging biomarkers.

radiotherapy (74–77). PX-866, a PI3K inhibitor with selectivity for p110α, is a biologically stable synthetic viridian related to wortmannin. PX-866 has demonstrated single agent anti-tumor activity in A549 human non-small cell lung cancer (NSCLC) and human ovarian cancer (OvCar-3) xenografts as well as increases in the anti-tumor effects of cisplatin and radiation treatment (73). In our group, preliminary data using PX-866 has shown a reduction in permeability 48 h post-therapy in HT-29 tumors (Fig. 5).

Another important target downstream in PI3K-AKT pathway that upregulates cell growth and proliferation is the mammalian target of rapamycin (mTOR). mTOR is a current target for anti-cancer therapies, such as rapamycin and it analogues (CC1779, Rad 001, AP23573 and AP23841). CCI-779 is the most extensively studied analogue with efficacy having been shown in Phase II clinical trials in patients with renal cell carcinomas and glioblastomas (78,79). Moreover, CCI-779 has demonstrated decreased growth in a range of tumors with PTEN mutations including breast and other cancer models (80–82).

A recent seminal paper by Rosen's group at Memorial showed that, when BAD is phosphorylated by AKT or MAP kinase, it is sequestered by the 14-3-3 protein, and prevented from inhibiting the anti-apoptotic BCL-2 and BCL-XL proteins (83). Hence, activation of MAPK through EGFR or activation of AKT through inhibition of PTEN will inhibit apoptosis. Rosen also showed that PTEN deficient breast cancer cells were resistant to gefitinib but were re-sensitized if PTEN activity was restored.

The use of molecular imaging in detecting early target inhibition in the PI3K-AKT pathway has been extremely limited. However, since the PI3K pathway directly targets glucose uptake and metabolism, there is significant potential, particularly in the area of functional imaging and the use of ^{18}FDG PET.

HYPOXIA INDUCIBLE FACTOR (HIF)

Oxygen homeostasis is a highly regulated process. Hypoxia Inducible Factor (HIF)-1 is recognized primarily for its role in the maintenance of oxygen and energy homeostasis. HIF-1 mediates a pleiotropic response to hypoxic stress by inducing more than 40 genes involved in energy metabolism, iron metabolism and angiogenesis (84). An increase in HIF-1α resulting from intratumoral hypoxia,

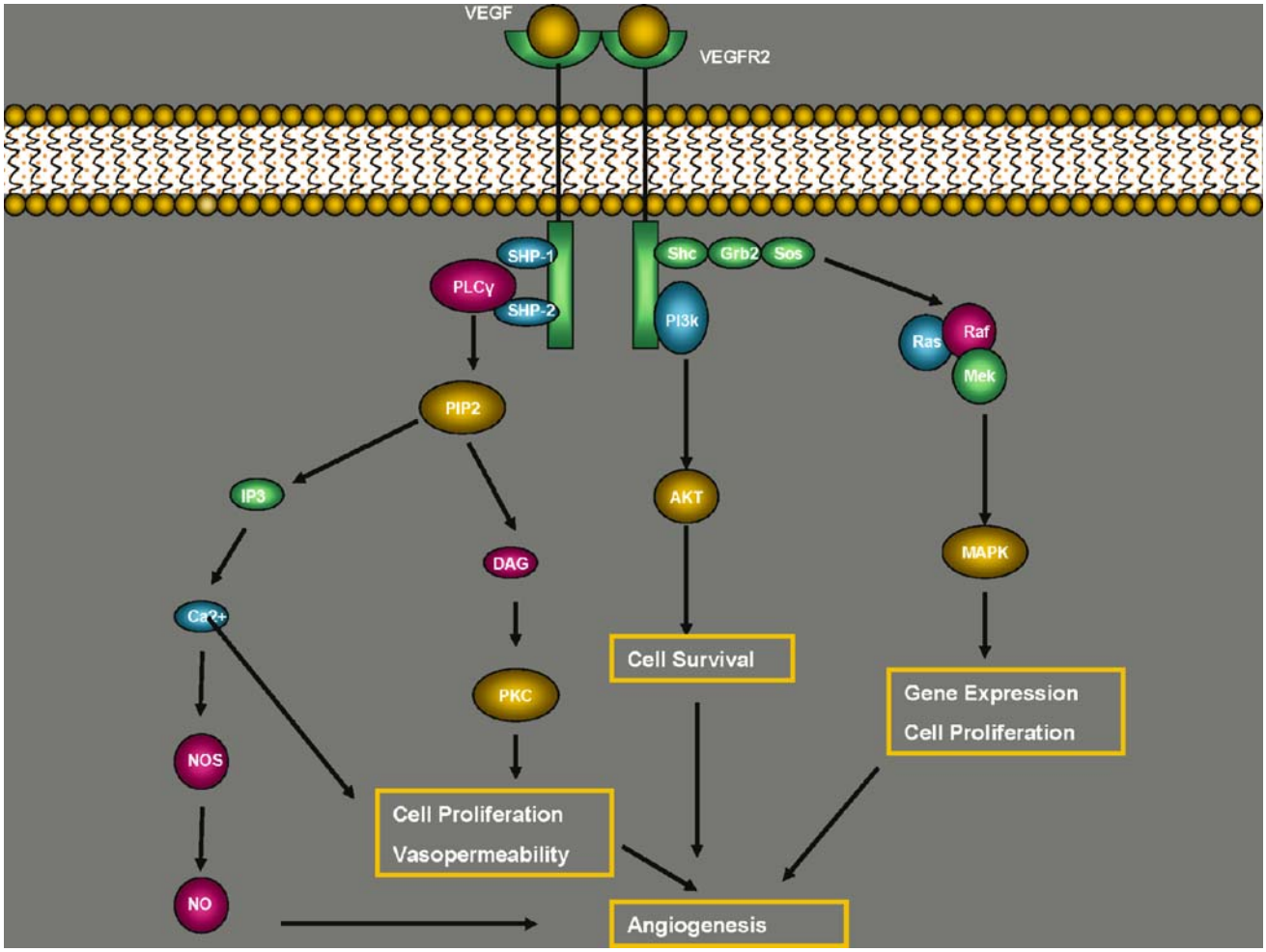

Fig. 7. VEGF Signaling and downstream effects of activation.

genetic alterations or a combination of both leads primarily to increased transcription of angiogenic genes (e.g., VEGF) and altered glucose metabolism (85).

HIF-1 is a heterodimer that functions as the master regulator of oxygen homeostasis. It is composed of two constitutively expressed HIF-1α and HIF-1β subunits that are basic helix-loop-helix-PAS domain proteins (86). HIF-1β is ubiquitously expressed whereas HIF-1α is destabilized under normoxic conditions. In the presence of oxygen, HIF-1α (120 kD) is regulated by prolyl hydroxylases that hydroxylate two specific proline residues (564 and 402) on HIF-1α (85,87,88). This enzymatic modification allows for the binding of the Von Hippel-Lindau (VHL) tumor suppressor protein, the recognition component for ubiquitin ligase, leading to immediate ubiquitination and proteasomal degradation of the α subunit (89–91). In normoxia, the half-life of HIF-1α is less than 10 min at which point the protein is almost completely undetectable (89). Under hypoxic conditions, oxygen availability is limited resulting in erythropoiesis through the production of erythropoietin (EPO) and in angiogenesis to increase oxygen delivery (92). Furthermore, the expression of certain glycolytic enzymes (aldolase A and C, enolase 1, hexokinase 1 and 3, lactate dehydrogenase A, phosphofructokinase L and phosphoglycerate kinase 1), glucose transporters (GLUT 1 and 3), and growth factors (insulin-like growth factor 2) are upregulated to adapt to the changing energy needs and to promote tumor cell survival (85). In hypoxia, the prolyl hydroxylases become inactivated, preventing the binding of VHL, resulting in HIF-1α escaping both ubiquitination and proteasomal degradation (91). HIF-1α is then transported to the nucleus where upon dimerization with HIF-1β an active transcription factor complex is formed that binds to regions of DNA known as hypoxia response element (HRE), an upstream promoter region of target genes (92).

Intratumoral hypoxia and genetic alterations including loss or inactivation of VHL, p53, or PTEN, or activation of Ras or pAKT can result in the overexpression or stabilization of HIF-1α in many cancers (93,94). Thus, HIF-1α can remain elevated even under normoxic conditions (95) and can be induced by a variety of other stimulants including nitric oxide (96), insulin-like growth factor (97,98), $HER2^{neu}$ (99) and prostaglandin E2 (100). In the setting of cancer, accumulation of HIF-1α protein is associated with highly aggressive tumors and a poorer patient prognosis (85). For instance, in both breast and brain tumors, a significant relationship exists between HIF-1α levels and tumor grade (101,102). The accumulation of HIF-1α can result in altered glucose metabolism and tumor progression resulting ultimately in treatment failure.

Targeted Therapy and Functional and Molecular Imaging

Targeting the HIF-1α signaling pathway to inhibit tumor progression is attractive as hypoxic tumors limit the effectiveness of chemo- and radiotherapies, and the fact that HIF-1α can be stabilized by a number of other factors, most of which are drug targets (103). These are shown in Fig. 6, along with the sequelae of HIF-1α activity, namely survival, glucose transport and expression of VEGF, which can be measured non-invasively with Diffusion-Weighted, FDG-PET, and DCE-MR imaging, respectively.

There are currently four major areas of research in hypoxia related drug therapy: direct inhibitors of HIF-1, indirect inhibitors of HIF-1 through other signaling cascades, hypoxia regulated genes and hypoxia activated agents (104). PX-478 has been the pioneer drug in demonstrating direct reductions in HIF expression (105). Additionally, 103D5R, a novel small molecule inhibitor of HIF-1α, has shown promise in directly inhibiting protein expression in xenografts (106).

Using PX-478, Jordan *et al.* (5) observed a dramatic reduction in tumor blood vessel permeability within 2 h, followed by a significant (almost 2-fold) increase in tumor diffusion (ADC) within 24 h of treatment. Tumor cellularity, estimated from ADC, was significantly decreased 24 h and 36 h after treatment. Based on these studies, Diffusion-Weighted and DCE MRI data will be collected from patients in the clinical trials of PX-478. Additional molecular and functional imaging of HIF-1α inhibitors has been limited.

VASCULAR ENDOTHELIAL GROWTH FACTOR (VEGF)

VEGF, a homodimeric glycoprotein with a molecular weight of 45 kD, is a key player in angiogenesis and in tumor progression. In the initial stages of tumor growth, tumor cells are fairly dormant with cellular proliferation being balanced by apoptotic rate (107). Tumors beyond 500 μm must be vascularized in order to avoid necrosis and/or apoptosis (108,109). As the tumor grows, it quickly outgrows its vasculature that supplies essential nutrients and oxygen. If an adequate blood supply cannot be found, the "angiogenic switch" will be triggered as a result of low pO_2, low pH and low glucose (110). The hypoxic tumor cell releases transcription factors such as hypoxia inducible factor that stimulate proangiogenic growth factors such as platelet-derived endothelial cell growth factors (PDGF), fibroblast growth factors (FGF), transforming growth factors (TGF), interleukins (IL) and vascular endothelial growth factors (VEGF) to be released. VEGF is normally expressed during embryogenesis (111–113), the reproductive cycle (114) and wound healing (115).

In the setting of cancer, VEGF plays a multifaceted role in tumor progression. Upon release, VEGF binds to two receptor tyrosine kinases (VEGF-1 and -2) triggering signaling cascades involved in angiogenesis and cell migration (Fig. 7). In addition to inducing the sprouting and growth of new blood vessels, VEGF increases vascular permeability allowing for the leakage of plasma proteins in tumors (116). Activated endothelial cells release matrix metalloproteases (117) that degrade the basement membrane and the extracellular matrix. Furthermore, VEGF protects the newly formed vasculature from destruction by inducing anti-apoptotic signals such as BCL-2 (118) and survivin (119). It is important to note that the newly formed vasculature is functionally and structurally distinct from normal tissue.

Imaging Has Shown Tumor Perfusion to Be Heterogenous

The homeostatic regulation of the vascular network is crucial toward maintaining tissue function (120). A mature vasculature must adapt to changing metabolic demands through adjustments in blood flow in vessels in order to provide adequate perfusion to maintain oxygen tensions, physiologic pH and adequate levels of glucose and other nutrients (121). This requires a highly coordinated system that is able to relay information both upstream and downstream of local conditions and respond via synchronized changes in diameters of vessels along flow pathways (120). Dysregulation of this system, as in solid tumors, lead to a chaotic vasculature containing regions of long, tortuous vessels coexisting with numerous short vessels and shunts (121,122). Specifically, features of a chaotic vasculature include: spatial heterogeneity and chaotic structures, arterio-venous shunts, acutely collapsed and transiently collapsing vessels, poorly differentiated, fragile and leaky vessels, and a vasculature unable to meet the demands of cancer cells (123). Consequently, blood flow and resistance in vessels become unbalanced contributing to heterogeneous perfusion (43). Paradoxically, heterogeneously perfused angiogenic tissue are not only poorly perfused but also hypoxic as a result of unbalanced resistance and blood flow through vessels stimulating even further VEGF production (122).

Targeted Therapy and Functional and Molecular Imaging

VEGF plays a crucial role in tumor growth and metastasis in many epithelial derived cancers including colorectal (124), breast (125), lung (126) and cervical (127). It is an attractive target as it can be altered without affecting normal physiology and be used as a prognostic indicator of angiogenesis (128). Additionally, since VEGF is a circulating molecule, penetrating the tumor is not crucial as in other drug therapies (128). Current anti-angiogenic therapies are targeted against either VEGF or its tyrosine kinase receptors. In 2004, the FDA approved the first anti-angiogenic drug (bevacizumab) to be used in combination with chemotherapy for metastatic colorectal cancer. In 2006, sunitinib received FDA approval for the treatment of metastatic renal cell carcinoma and gastrointestinal stromal tumors (129). Other experimental anti-angiogenic drugs include AG-013736, Bay 57-9352, SU5416, SU6668, PTK787, ZD6474 and DC101 all targeting tyrosine kinase receptors. Dynamic Contrast Enhanced MRI has played a strong supportive role in assessing tumor vascularity and permeability following treatment of agents such as bevacizumab (130), PTK787 (131,132), AG-013736 (133,134), and sunitinib (135).

Bevacizumab, a humanized monoclonal antibody against VEGF, has demonstrated the greatest success in both human and animal models. In various clinical phase trials, bevacizumab in combination with chemotherapy has demonstrated increased response rates, median time to disease progression and median survival time (136,137) in patients with untreated

metastatic colorectal cancer. In animal xenograft models, bevacizumab has demonstrated a marked decrease in vascular density, permeability and interstitial pressure (5,138). DCE-MRI has supported these data through vascular parameters that indicated reduced angiogenesis (5,130,139).

PTK-787/ZK222584, as part of phase I clinical trials has shown reductions in flow, permeability and vascular surface area in colon cancer patients (5,131,132). AG-013736, an oral angiogenesis inhibitor, has also demonstrated a decrease in tumor vascular parameters in patients with advanced solid tumors following acute dosing (133). Li *et al.* (134) gave further credence to utilizing DCE-MRI through assessment of the heterogeneity in the angiogenic response to AG-013736 by voxel analysis.

Sunitinib, a multi-targeted tyrosine kinase inhibitor, demonstrated early anti-angiogenic effects using DCE-MRI following a single dose administration. A 42% and a 31% decrease was observed in vascular permeability and in initial area under the concentration time curve using a macromolecular (Gd-DTPA-Albumin) and low molecular weight (Gd-DTPA) contrast agent respectively (135). This is particularly promising as the current clinical contrast agents are low molecular weight agents.

The use of FDG-PET in detecting response to anti-VEGF therapies has been limited. Jennens *et al.* (140) demonstrated early metabolic response to SU5416 (semaxanib), a potent VEGF receptor inhibitor, on a FDG-PET scan within 2 weeks of therapy in a patient with probable Von Hippel Lindau syndrome and metastatic renal cell cancer. Further reduction in both extent and intensity of FDG uptake in all tumor sites was observed at 4 weeks and a complete metabolic response at 12 months following treatment. This study demonstrates the potentially significant role of FDG-PET as a biomarker in the early response to anti-VEGF therapies.

CONCLUSIONS

The rise in deaths due to cancer in conjunction with rising drug development costs have forced the research community to think outside of the box. A majority of the development costs are tied up in clinical trials in order to verify safety, sensitivity, efficacy and reproducibility, of which none can be compromised. Therefore, the goal has been to make clinical trials more efficient and thereby mitigate associated costs of drug development and clinical trials. Imaging biomarkers, particularly functional and molecular imaging, have the potential to do this through validation of drug targets, confirming mechanisms of action and theragnostically predicting early responders to drug treatment.

Despite the promise and progress of molecular and functional imaging, imaging has not been incorporated into clinical trial designs and has seen only limited action in experimental animal studies. The existing bodies of work, however, have demonstrated significant potential for imaging in acquiring information regarding cellularity, metabolism and vasculature using Diffusion-Weighted MRI, FDG-PET, and DCE MRI respectively. The three targets (PI3K-AKT, HIF-1α, and VEGF) discussed in this review have significance in regards to their role in tumor progression but also in their potential to be used by the aforementioned imaging endpoints. Ultimately, application of molecular and functional imaging can be expected to result in significant savings in time and costs during all stages of drug development and testing.

REFERENCES

1. W. R. Parulekar and E. A. Eisenhauer. Phase I trial design for solid tumor studies of targeted, non-cytotoxic agents: theory and practice. *J. Natl. Cancer Inst.* **96**:990–997 (2004).
2. R. G. Blasberg. Molecular imaging and cancer. *Mol. Cancer Ther.* **2**:335–343 (2003).
3. J. L. Evelhoch, R. J. Gillies, G. S. Karczmar, J. A. Koutcher, R. J. Maxwell, O. Nalcioglu, N. Raghunand, S. M. Ronen, B. D. Ross, and H. M. Swartz. Applications of magnetic resonance in model systems: cancer therapeutics. *Neoplasia* **2**:152–165 (2000).
4. B. F. Jordan, K. Black, I. F. Robey, M. Runquist, G. Powis, and R. J. Gillies. Metabolite changes in HT-29 xenograft tumors following HIF-1alpha inhibition with PX-478 as studied by MR spectroscopy *in vivo* and *ex vivo*. *NMR Biomed.* **18**(7):430–439 (2005).
5. B. F. Jordan, M. Runquist, N. Raghunand, A. Baker, R. Williams, L. Kirkpatrick, G. Powis, and R. J. Gillies. Dynamic contrast-enhanced and diffusion MRI show rapid and dramatic changes in tumor microenvironment in response to inhibition of HIF-1alpha using PX-478. *Neoplasia* **7**:475–485 (2005).
6. G. J. Kelloff, K. A. Krohn, S. M. Larson, R. Weissleder, D. A. Mankoff, J. M. Hoffman, J. M. Link, K. Z. Guyton, W. C. Eckelman, H. I. Scher, J. O'Shaughnessy, B. D. Cheson, C. C. Sigman, J. L. Tatum, G. Q. Mills, D. C. Sullivan, and J. Woodcock. The progress and promise of molecular imaging probes in oncologic drug development. *Clin. Cancer Res.* **11**:7967–7985 (2005).
7. R. J. Gillies, Z. M. Bhujwalla, J. Evelhoch, M. Garwood, M. Neeman, S. P. Robinson, C. H. Sotak, and B. Van Der Sanden. Applications of magnetic resonance in model systems: tumor biology and physiology. *Neoplasia* **2**:139–151 (2000).
8. J. P. Galons, D. L. Morse, D. R. Jennings, and R. J. Gillies. Diffusion-weighted MRI and response to anti-cancer therapies. *Isr. J. Chem.* **43**:91–101 (2003).
9. T. L. Chenevert, P. E. McKeever, and B. D. Ross. Monitoring early response of experimental brain tumors to therapy using diffusion magnetic resonance imaging. *Clin. Cancer Res.* **3**:1457–1466 (1997).
10. Y. Mardor, Y. Roth, Z. Lidar, T. Jonas, R. Pfeffer, S. E. Maier, M. Faibel, D. Nass, M. Hadani, A. Orenstein, J. S. Cohen, and Z. Ram. Monitoring response to convection-enhanced taxol delivery in brain tumor patients using diffusion-weighted magnetic resonance imaging. *Cancer Res.* **61**:4971–4973 (2001).
11. Y. Mardor, R. Pfeffer, R. Spiegelmann, Y. Roth, S. E. Maier, O. Nissim, R. Berger, A. Glicksman, J. Baram, A. Orenstein, J. S. Cohen, and T. Tichler. Early detection of response to radiation therapy in patients with brain malignancies using conventional and high b-value diffusion-weighted magnetic resonance imaging. *J. Clin. Oncol.* **21**:1094–1100 (2003).
12. D. E. Hall, B. A. Moffat, J. Stojanovska, T. D. Johnson, Z. Li, D. A. Hamstra, A. Rehemtulla, T. L. Chenevert, J. Carter, D. Pietronigro, and B. D. Ross. Therapeutic efficacy of DTI-015 using diffusion magnetic resonance imaging as an early surrogate marker. *Clin. Cancer Res.* **10**:7852–7859 (2004).
13. K. C. Lee, D. E. Hall, B. A. Hoff, B. A. Moffat, S. Sharma, T. L. Chenevert, C. R. Meyer, W. R. Leopold, T. D. Johnson, R. V. Mazurchuk, A. Rehemtulla, and B. D. Ross. Dynamic imaging of emerging resistance during cancer therapy. *Cancer Res.* **66**:4687–4692 (2006).
14. B. A. Moffat, T. L. Chenevert, T. S. Lawrence, C. R. Meyer, T. D. Johnson, Q. Dong, C. Tsien, S. Mukherji, D. J. Quint, S. S. Gebarski, P. L. Robertson, L. R. Junck, A. Rehemtulla, and B. D. Ross. Functional diffusion map: a noninvasive MRI biomarker for early stratification of clinical brain tumor response. *Proc. Natl. Acad. Sci. USA.* **102**:5524–5529 (2005).
15. P. A. Hein, C. Kremser, W. Judmaier, J. Griebel, K. P. Pfeiffer, A. Kreczy, E. B. Hug, P. Lukas, and A. F. DeVries. Diffusion-weighted magnetic resonance imaging for monitoring diffusion changes in rectal carcinoma during combined, preoperative

chemoradiation: preliminary results of a prospective study. *Eur. J. Radiol.* **45**:214–222 (2003).
16. M. Uhl, U. Saueressig, M. Buirenvan, U. Kontny, C. Niemeyer, G. Kohler, K. Ilyasov, and M. Langer. Osteosarcoma: preliminary results of *in vivo* assessment of tumor necrosis after chemotherapy with diffusion- and perfusion-weighted magnetic resonance imaging. *Invest. Radiol.* **41**:618–623 (2006).
17. R. J. Theilmann, R. Borders, T. P. Trouard, G. Xia, E. Outwater, J. Ranger-Moore, R. J. Gillies, and A. Stopeck. Changes in water mobility measured by diffusion MRI predict response of metastatic breast cancer to chemotherapy. *Neoplasia* **6**:831–837 (2004).
18. A. Dzik-Jurasz, C. Domenig, M. George, J. Wolber, A. Padhani, G. Brown, and S. Doran. Diffusion MRI for prediction of response of rectal cancer to chemoradiation. *Lancet* **360**:307–308 (2002).
19. L. Lemaire, F. A. Howe, L. M. Rodrigues, and J. R. Griffiths. Assessment of induced rat mammary tumour response to chemotherapy using the apparent diffusion coefficient of tissue water as determined by diffusion-weighted 1H-NMR spectroscopy *in vivo*. *Magma* **8**:20–26 (1999).
20. M. Zhao, J. G. Pipe, J. Bonnett, and J. L. Evelhoch. Early detection of treatment response by diffusion-weighted 1H-NMR spectroscopy in a murine tumour *in vivo*. *Br. J. Cancer* **73**:61–64 (1996).
21. D. A. Beauregard, P. E. Thelwall, D. J. Chaplin, S. A. Hill, G. E. Adams, and K. M. Brindle. Magnetic resonance imaging and spectroscopy of combretastatin A4 prodrug-induced disruption of tumour perfusion and energetic status. *Br. J. Cancer* **77**:1761–1767 (1998).
22. J. P. Galons, M. I. Altbach, G. D. Paine-Murrieta, C. W. Taylor, and R. J. Gillies. Early increases in breast tumor xenograft water mobility in response to paclitaxel therapy detected by non-invasive diffusion magnetic resonance imaging. *Neoplasia* **1**:113–117 (1999).
23. D. Jennings, B. N. Hatton, J. Guo, J. P. Galons, T. P. Trouard, N. Raghunand, J. Marshall, and R. J. Gillies. Early response of prostate carcinoma xenografts to docetaxel chemotherapy monitored with diffusion MRI. *Neoplasia* **4**:255–262 (2002).
24. H. C. Thoeny, F. De Keyzer, F. Chen, V. Vandecaveye, E. K. Verbeken, B. Ahmed, X. Sun, Y. Ni, H. Bosmans, R. Hermans, A. van Oosterom, G. Marchal, and W. Landuyt. Diffusion-weighted magnetic resonance imaging allows noninvasive *in vivo* monitoring of the effects of combretastatin a-4 phosphate after repeated administration. *Neoplasia* **7**:779–787 (2005).
25. A. M. Chinnaiyan, U. Prasad, S. Shankar, D. A. Hamstra, M. Shanaiah, T. L. Chenevert, B. D. Ross, and A. Rehemtulla. Combined effect of tumor necrosis factor-related apoptosis-inducing ligand and ionizing radiation in breast cancer therapy. *Proc. Natl. Acad. Sci. USA.* **97**:1754–1759 (2000).
26. E. Rustamzadeh, W. A. Hall, D. A. Todhunter, W. C. Low, H. Liu, A. Panoskaltsis-Mortari, and D. A. Vallera. Intracranial therapy of glioblastoma with the fusion protein DTIL13 in immunodeficient mice. *Int. J. Cancer* **118**:2594–2601 (2006).
27. K. Turetschek, E. Floyd, D. M. Shames, T. P. Roberts, A. Preda, V. Novikov, C. Corot, W. O. Carter, and R. C. Brasch. Assessment of a rapid clearance blood pool MR contrast medium (P792) for assays of microvascular characteristics in experimental breast tumors with correlations to histopathology. *Magn. Reson. Med.* **45**:880–886 (2001).
28. B. A. Birnbaum, J. C. Weinreb, M. P. Fernandez, J. J. Brown, N. M. Rofsky, and S. W. Young. Comparison of contrast enhanced CT and Mn-DPDP enhanced MRI for detection of focal hepatic lesions. Initial findings. *Clin. Imaging* **18**:21–27 (1994).
29. A. M. Lutz, J. K. Willmann, K. Goepfert, B. Marincek, and D. Weishaupt. Hepatocellular carcinoma in cirrhosis: enhancement patterns at dynamic gadolinium- and superparamagnetic iron oxide-enhanced T1-weighted MR imaging. *Radiology* **237**:520–528 (2005).
30. P. L. Choyke, A. J. Dwyer, and M. V. Knopp. Functional tumor imaging with dynamic contrast-enhanced magnetic resonance imaging. *J. Magn. Reson. Imaging* **17**:509–520 (2003).
31. M. V. Knopp, F. L. Giesel, H. Marcos, H. von Tengg-Kobligk, and P. Choyke. Dynamic contrast-enhanced magnetic resonance imaging in oncology. *Top Magn. Reson. Imaging* **12**:301–308 (2001).
32. W.R. Hendee and E.R. Ritenour. Medical Imaging Physics, Mobsy, St. Louis, 1992.
33. A. Quon and S. S. Gambhir. FDG-PET and beyond: molecular breast cancer imaging. *J. Clin. Oncol.* **23**:1664–1673 (2005).
34. R. Bos, J. J. van Der Hoeven, E. van Der Wall, P. van Der Groep, P. J. van Diest, E. F. Comans, U. Joshi, G. L. Semenza, O. S. Hoekstra, A. A. Lammertsma, and C. F. Molthoff. Biologic correlates of (18)fluorodeoxyglucose uptake in human breast cancer measured by positron emission tomography. *J. Clin. Oncol.* **20**:379–387 (2002).
35. B. M. Burt, J. L. Humm, D. A. Kooby, O. D. Squire, S. Mastorides, S. M. Larson, and Y. Fong. Using positron emission tomography with [(18)F]FDG to predict tumor behavior in experimental colorectal cancer. *Neoplasia* **3**:189–195 (2001).
36. R. A. Gatenby and R. J. Gillies. Why do cancers have high aerobic glycolysis?. *Nat. Rev. Cancer* **4**:891–899 (2004).
37. M. Kunkel, T. E. Reichert, P. Benz, H. A. Lehr, J. H. Jeong, S. Wieand, P. Bartenstein, W. Wagner, and T. L. Whiteside. Overexpression of Glut-1 and increased glucose metabolism in tumors are associated with a poor prognosis in patients with oral squamous cell carcinoma. *Cancer* **97**:1015–1024 (2003).
38. E. Mochiki, H. Kuwano, H. Katoh, T. Asao, N. Oriuchi, and K. Endo. valuation of 18F-2-deoxy-2-fluoro-D-glucose positron emission tomography for gastric cancer. *World J. Surg.* **28**:247–253 (2004).
39. A. Gennari, S. Donati, B. Salvadori, A. Giorgetti, P. A. Salvadori, O. Sorace, G. Puccini, P. Pisani, M. Poli, D. Dani, E. Landucci, G. Mariani, and P. F. Conte. Role of 2-[18F]-fluorodeoxyglucose (FDG) positron emission tomography (PET) in the early assessment of response to chemotherapy in metastatic breast cancer patients. *Clin. Breast Cancer* **1**:156–161 (2000); (discussion 162–163).
40. R. Kumar and A. Alavi. Fluorodeoxyglucose-PET in the management of breast cancer. *Radiol. Clin. North Am.* **42**:1113–1122 (2004), ix.
41. J. S. Ryu, N. C. Choi, A. J. Fischman, T. J. Lynch, and D. J. Mathisen. FDG-PET in staging and restaging non-small cell lung cancer after neoadjuvant chemoradiotherapy: correlation with histopathology. *Lung Cancer* **35**:179–187 (2002).
42. A. Dimitrakopoulou-Strauss, L. G. Strauss, and J. Rudi. PET-FDG as predictor of therapy response in patients with colorectal carcinoma. *Q. J. Nucl. Med.* **47**:8–13 (2003).
43. R. J. Gillies, P. A. Schornack, T. W. Secomb, and N. Raghunand. Causes and effects of heterogeneous perfusion in tumors. *Neoplasia* **1**:197–207 (1999).
44. H. E. Daldrup-Link, D. M. Shames, M. Wendland, A. Muhler, A. Gossmann, W. Rosenau, and R. C. Brasch. Comparison of Gadomer-17 and gadopentetate dimeglumine for differentiation of benign from malignant breast tumors with MR imaging. *Acad. Radiol.* **7**:934–944 (2000).
45. M. Y. Su, Z. Wang, P. M. Carpenter, X. Lao, A. Muhler, and O. Nalcioglu. Characterization of N-ethyl-N-nitrosourea-induced malignant and benign breast tumors in rats by using three MR contrast agents. *J. Magn. Reson. Imaging* **9**:177–186 (1999).
46. R. J. Maxwell, J. Wilson, V. E. Prise, B. Vojnovic, G. J. Rustin, M. A. Lodge, and G. M. Tozer. Evaluation of the anti-vascular effects of combretastatin in rodent tumours by dynamic contrast enhanced MRI. *NMR Biomed.* **15**:89–98 (2002).
47. C. Hayes, A. R. Padhani, and M. O. Leach. Assessing changes in tumour vascular function using dynamic contrast-enhanced magnetic resonance imaging. *NMR Biomed.* **15**:154–163 (2002).
48. M. Y. Su, Y. C. Cheung, J. P. Fruehauf, H. Yu, O. Nalcioglu, E. Mechetner, A. Kyshtoobayeva, S. C. Chen, S. Hsueh, C. E. McLaren, and Y. L. Wan. Correlation of dynamic contrast enhancement MRI parameters with microvessel density and VEGF for assessment of angiogenesis in breast cancer. *J. Magn. Reson. Imaging* **18**:467–477 (2003).
49. K. Turetschek, A. Preda, V. Novikov, R. C. Brasch, H. J. Weinmann, P. Wunderbaldinger, and T. P. Roberts. Tumor microvascular changes in antiangiogenic treatment: assessment by magnetic resonance contrast media of different molecular weights. *J. Magn. Reson. Imaging* **20**:138–144 (2004).
50. M. Port, C. Corot, I. Raynal, J. M. Idee, A. Dencausse, E. Lancelot, D. Meyer, B. Bonnemain, and J. Lautrou. Physicochemical and biological evaluation of P792, a rapid-clearance

blood-pool agent for magnetic resonance imaging. *Invest. Radiol.* **36**:445–454 (2001).
51. A. Mavi, M. Urhan, J. Q. Yu, H. Zhuang, M. Houseni, T. F. Cermik, D. Thiruvenkatasamy, B. Czerniecki, M. Schnall, and A. Alavi. Dual time point 18F-FDG PET imaging detects breast cancer with high sensitivity and correlates well with histologic subtypes. *J. Nucl. Med.* **47**:1440–1446 (2006).
52. J. Tseng, L. K. Dunnwald, E. K. Schubert, J. M. Link, S. Minoshima, M. Muzi, and D. A. Mankoff. 18F-FDG kinetics in locally advanced breast cancer: correlation with tumor blood flow and changes in response to neoadjuvant chemotherapy. *J. Nucl. Med.* **45**:1829–1837 (2004).
53. K. A. Phillips, S. Van Bebber, and A. M. Issa. Diagnostics and biomarker development: priming the pipeline. *Nat. Rev. Drug Discov.* **5**:463–469 (2006).
54. J. A. DiMasi, R. W. Hansen, and H. G. Grabowski. The price of innovation: new estimates of drug development costs. *J. Health Econ.* **22**:151–185 (2003).
55. E. Nadler, B. Eckert, and P. J. Neumann. Do oncologists believe new cancer drugs offer good value?. *Oncologist* **11**:90–95 (2006).
56. R. Weissleder. Molecular imaging in cancer. *Science* **312**:1168–1171 (2006).
57. T. Sjoblom, S. Jones, L. D. Wood, D. W. Parsons, J. Lin, T. Barber, D. Mandelker, R. J. Leary, J. Ptak, N. Silliman, S. Szabo, P. Buckhaults, C. Farrell, P. Meeh, S. D. Markowitz, J. Willis, D. Dawson, J. K. Willson, A. F. Gazdar, J. Hartigan, L. Wu, C. Liu, G. Parmigiani, B. H. Park, K. E. Bachman, N. Papadopoulos, B. Vogelstein, K. W. Kinzler, and V. E. Velculescu. The consensus coding sequences of human breast and colorectal cancers. *Science* **7**:7 (2006).
58. R. Simon and A. Maitournam. Evaluating the efficiency of targeted designs for randomized clinical trials. *Clin. Cancer Res.* **10**:6759–6763 (2004).
59. R. J. Gillies and D. L. Morse. *In vivo* magnetic resonance spectroscopy in cancer. *Annu. Rev. Biomed. Eng.* **7**:287–326 (2005).
60. J. A. DiMasi. The value of improving the productivity of the drug development process: faster times and better decisions. *Pharmacoeconomics* **20**:1–10 (2002).
61. J. Y. Blay, A. CesneLe, L. Alberti, and I. Ray-Coquart. Targeted cancer therapies. *Bull. Cancer* **92**:E13–E18 (2005).
62. S. Faivre, S. Djelloul, and E. Raymond. New paradigms in anticancer therapy: targeting multiple signaling pathways with kinase inhibitors. *Semin. Oncol.* **33**:407–420 (2006).
63. S. R. Datta, A. Brunet, and M. E. Greenberg. Cellular survival: a play in three Akts. *Genes Dev.* **13**:2905–2929 (1999).
64. I. Vivanco and C. L. Sawyers. The phosphatidylinositol 3-Kinase AKT pathway in human cancer. *Nat. Rev. Cancer* **2**:489–501 (2002).
65. P. Blume-Jensenand and T. Hunter. Oncogenic kinase signalling. *Nature* **411**:355–365 (2001).
66. N. Gao, Z. Zhang, B. H. Jiang, and X. Shi. Role of PI3K/AKT/mTOR signaling in the cell cycle progression of human prostate cancer. *Biochem. Biophys. Res. Commun.* **310**:1124–1132 (2003).
67. M. Osaki, M. Oshimura, and H. Ito. PI3K-Akt pathway: its functions and alterations in human cancer. *Apoptosis* **9**:667–676 (2004).
68. A. Di Cristofano, P. Kotsi, Y. F. Peng, C. Cordon-Cardo, K. B. Elkon, and P. P. Pandolfi. Impaired Fas response and autoimmunity in Pten+/− mice. *Science* **285**:2122–2125 (1999).
69. K. M. Nicholson and N. G. Anderson. The protein kinase B/Akt signalling pathway in human malignancy. *Cell. Signal.* **14**:381–395 (2002).
70. B. T. Hennessy, D. L. Smith, P. T. Ram, Y. Lu, and G. B. Mills. Exploiting the PI3K/AKT pathway for cancer drug discovery. *Nat. Rev. Drug Discov.* **4**:988–1004 (2005).
71. D. R. Alessi and P. Cohen. Mechanism of activation and function of protein kinase B. *Curr. Opin. Genet. Dev.* **8**:55–62 (1998).
72. P. J. Coffer, J. Jin, and J. R. Woodgett. Protein kinase B (c-Akt): a multifunctional mediator of phosphatidylinositol 3-kinase activation. *Biochem. J.* **335**:1–13 (1998).
73. N. T. Ihle, R. Williams, S. Chow, W. Chew, M. I. Berggren, G. Paine-Murrieta, D. J. Minion, R. J. Halter, P. Wipf, R. Abraham, L. Kirkpatrick, and G. Powis. Molecular pharmacology and antitumor activity of PX-866, a novel inhibitor of phosphoinositide-3-kinase signaling. *Mol. Cancer Ther.* **3**:763–772 (2004).
74. A. R. Gottschalk, A. Doan, J. L. Nakamura, D. Stokoe, and D. A. Haas-Kogan. Inhibition of phosphatidylinositol-3-kinase causes increased sensitivity to radiation through a PKB-dependent mechanism. *Int. J. Radiat. Oncol. Biol. Phys.* **63**:1221–1227 (2005).
75. L. Hu, C. Zaloudek, G. B. Mills, J. Gray, and R. B. Jaffe. *In vivo* and *in vitro* ovarian carcinoma growth inhibition by a phosphatidylinositol 3-kinase inhibitor (LY294002). *Clin. Cancer Res.* **6**:880–886 (2000).
76. S. S. Ng, M. S. Tsao, T. Nicklee, and D. W. Hedley. Wortmannin inhibits pkb/akt phosphorylation and promotes gemcitabine antitumor activity in orthotopic human pancreatic cancer xenografts in immunodeficient mice. *Clin. Cancer Res.* **7**:3269–3275 (2001).
77. K. E. Rosenzweig, M. B. Youmell, S. T. Palayoor, and B. D. Price. Radiosensitization of human tumor cells by the phosphatidylinositol3-kinase inhibitors wortmannin and LY294002 correlates with inhibition of DNA-dependent protein kinase and prolonged G2-M delay. *Clin. Cancer Res.* **3**:1149–1156 (1997).
78. M. B. Atkins, M. Hidalgo, W. M. Stadler, T. F. Logan, J. P. Dutcher, G. R. Hudes, Y. Park, S. H. Liou, B. Marshall, J. P. Boni, G. Dukart, and M. L. Sherman. Randomized phase II study of multiple dose levels of CCI-779, a novel mammalian target of rapamycin kinase inhibitor, in patients with advanced refractory renal cell carcinoma. *J. Clin. Oncol.* **22**:909–918 (2004).
79. E. Galanis, J. C. Buckner, M. J. Maurer, J. I. Kreisberg, K. Ballman, J. Boni, J. M. Peralba, R. B. Jenkins, S. R. Dakhil, R. F. Morton, K. A. Jaeckle, B. W. Scheithauer, J. Dancey, M. Hidalgo, and D. J. Walsh. Phase II trial of temsirolimus (CCI-779) in recurrent glioblastoma multiforme: a North Central Cancer Treatment Group Study. *J. Clin. Oncol.* **23**:5294–5304 (2005).
80. L. A. DeGraffenried, L. Fulcher, W. E. Friedrichs, V. Grunwald, R. B. Ray, and M. Hidalgo. Reduced PTEN expression in breast cancer cells confers susceptibility to inhibitors of the PI3 kinase/Akt pathway. *Ann. Oncol.* **15**:1510–1516 (2004).
81. M. S. Neshat, I. K. Mellinghoff, C. Tran, B. Stiles, G. Thomas, R. Petersen, P. Frost, J. J. Gibbons, H. Wu, and C. L. Sawyers. Enhanced sensitivity of PTEN-deficient tumors to inhibition of FRAP/mTOR. *Proc. Natl. Acad. Sci. USA.* **98**:10314–10319 (2001).
82. K. Podsypanina, R.T. Lee, C. Politis, I. Hennessy, A. Crane, J. Puc, M. Neshat, H. Wang, L. Yang, J. Gibbons, P. Frost, V. Dreisbach, J. Blenis, Z. Gaciong, P. Fisher, C. Sawyers, L. Hedrick-Ellenson, and R. Parsons. An inhibitor of mTOR reduces neoplasia and normalizes p70/S6 kinase activity in Pten+/− mice. *Proc. Natl. Acad. Sci. USA.* **98**:10320–10325 (2001).
83. Q. B. She, D. B. Solit, Q. Ye, K. E. O'Reilly, J. Lobo, and N. Rosen. The BAD protein integrates survival signaling by EGFR/MAPK and PI3K/Akt kinase pathways in PTEN-deficient tumor cells. *Cancer Cell* **8**:287–297 (2005).
84. G. L. Semenza. Hypoxia-inducible factor 1: oxygen homeostasis and disease pathophysiology. *Trends Mol. Med.* **7**:345–350 (2001).
85. G. L. Semenza. HIF-1 and tumor progression: pathophysiology and therapeutics. *Trends Mol. Med.* **8**:S62–S67 (2002).
86. G. L. Wang, B. H. Jiang, E. A. Rue, and G. L. Semenza. Hypoxia-inducible factor 1 is a basic-helix-loop-helix-PAS heterodimer regulated by cellular O2 tension. *Proc. Natl. Acad. Sci. USA.* **92**:5510–5514 (1995).
87. A. C. Epstein, J. M. Gleadle, L. A. McNeill, K. S. Hewitson, J. O'Rourke, D. R. Mole, M. Mukherji, E. Metzen, M. I. Wilson, A. Dhanda, Y. M. Tian, N. Masson, D. L. Hamilton, P. Jaakkola, R. Barstead, J. Hodgkin, P. H. Maxwell, C. W. Pugh, C. J. Schofield, and P. J. Ratcliffe. C. elegans EGL-9 and mammalian homologs define a family of dioxygenases that regulate HIF by prolyl hydroxylation. *Cell* **107**:43–54 (2001).

88. M. Ivan, K. Kondo, H. Yang, W. Kim, J. Valiando, M. Ohh, A. Salic, J. M. Asara, W. S. Lane, and W. G. Kaelin Jr. HIFalpha targeted for VHL-mediated destruction by proline hydroxylation: implications for O2 sensing. *Science* **292**:464–468 (2001).
89. Y. S. Chun, M. S. Kim, and J. W. Park. Oxygen-dependent and -independent regulation of HIF-1alpha. *J. Korean Med. Sci.* **17**:581–588 (2002).
90. L. E. Huang, J. Gu, M. Schau, and H. F. Bunn. Regulation of hypoxia-inducible factor 1alpha is mediated by an O2-dependent degradation domain via the ubiquitin-proteasome pathway. *Proc. Natl. Acad. Sci. USA.* **95**:7987–7992 (1998).
91. P. H. Maxwell, M. S. Wiesener, G. W. Chang, S. C. Clifford, E. C. Vaux, M. E. Cockman, C. C. Wykoff, C. W. Pugh, E. R. Maher, and P. J. Ratcliffe. The tumour suppressor protein VHL targets hypoxia-inducible factors for oxygen-dependent proteolysis. *Nature* **399**:271–275 (1999).
92. A. Zagorska and J. Dulak. HIF-1: the knowns and unknowns of hypoxia sensing. *Acta Biochim. Pol.* **51**:563–585 (2004).
93. K. L. Talks, H. Turley, K. C. Gatter, P. H. Maxwell, C. W. Pugh, P. J. Ratcliffe, and L. Harris. The expression and distribution of the hypoxia-inducible factors HIF-1alpha and HIF-2alpha in normal human tissues, cancers, and tumor-associated macrophages. *Am. J. Pathol.* **157**:411–421 (2000).
94. H. Zhong, A. M. MarzoDe, E. Laughner, M. Lim, D. A. Hilton, D. Zagzag, P. Buechler, W. B. Isaacs, G. L. Semenza, and J. W. Simons. Overexpression of hypoxia-inducible factor 1alpha in common human cancers and their metastases. *Cancer Res.* **59**:5830–5835 (1999).
95. I. F. Robey, A. D. Lien, S. J. Welsh, B. K. Baggett, and R. J. Gillies. Hypoxia-inducible factor-1alpha and the glycolytic phenotype in tumors. *Neoplasia* **7**:324–330 (2005).
96. K. Kasuno, S. Takabuchi, K. Fukuda, S. Kizaka-Kondoh, J. Yodoi, T. Adachi, G. L. Semenza, and K. Hirota. Nitric oxide induces hypoxia-inducible factor 1 activation that is dependent on MAPK and phosphatidylinositol 3-kinase signaling. *J. Biol. Chem.* **279**:2550–2558 (2004). Epub 2003 Nov 4.
97. R. Fukuda, K. Hirota, F. Fan, Y. D. Jung, L. M. Ellis, and G. L. Semenza. Insulin-like growth factor 1 induces hypoxia-inducible factor 1-mediated vascular endothelial growth factor expression, which is dependent on MAP kinase and phosphatidylinositol 3-kinase signaling in colon cancer cells. *J. Biol. Chem.* **277**:38205–38211 (2002).
98. C. Treins, S. Giorgetti-Peraldi, J. Murdaca, G. L. Semenza, and E. Van Obberghen. Insulin stimulates hypoxia-inducible factor 1 through a phosphatidylinositol 3-kinase/target of rapamycin-dependent signaling pathway. *J. Biol. Chem.* **277**:27975–27981 (2002).
99. E. Laughner, P. Taghavi, K. Chiles, P. C. Mahon, and G. L. Semenza. HER2 (neu) signaling increases the rate of hypoxia-inducible factor 1alpha (HIF-1alpha) synthesis: novel mechanism for HIF-1-mediated vascular endothelial growth factor expression. *Mol. Cell Biol.* **21**:3995–4004 (2001).
100. R. Fukuda, B. Kelly, and G. L. Semenza. Vascular endothelial growth factor gene expression in colon cancer cells exposed to prostaglandin E2 is mediated by hypoxia-inducible factor 1. *Cancer Res.* **63**:2330–2334 (2003).
101. R. Bos, H. Zhong, C. F. Hanrahan, E. C. Mommers, G. L. Semenza, H. M. Pinedo, M. D. Abeloff, J. W. Simons, P. J. van Diest, and E. van der Wall. Levels of hypoxia-inducible factor-1 alpha during breast carcinogenesis. *J. Natl. Cancer Inst.* **93**:309–314 (2001).
102. D. Zagzag, H. Zhong, J. M. Scalzitti, E. Laughner, J. W. Simons, and G. L. Semenza. Expression of hypoxia-inducible factor 1alpha in brain tumors: association with angiogenesis, invasion, and progression. *Cancer* **88**:2606–2618 (2000).
103. G. L. Semenza. Targeting HIF-1 for cancer therapy. *Nat. Rev. Cancer* **3**:721–732 (2003).
104. K. Lee, R. A. Roth, and J. J. Lapres. Hypoxia, drug therapy and toxicity. *Pharmacol. Ther.* **11**:11 (2006).
105. S. Welsh, R. Williams, L. Kirkpatrick, G. Paine-Murrieta, and G. Powis. Antitumor activity and pharmacodynamic properties of PX-478, an inhibitor of hypoxia-inducible factor-1alpha. *Mol. Cancer Ther.* **3**:233–244 (2004).
106. C. Tan, R. G. Noronhade, A. J. Roecker, B. Pyrzynska, F. Khwaja, Z. Zhang, H. Zhang, Q. Teng, A. C. Nicholson, P. Giannakakou, W. Zhou, J. J. Olson, M. M. Pereira, K. C. Nicolaou, and E. G. Van Meir. Identification of a novel small-molecule inhibitor of the hypoxia-inducible factor 1 pathway. *Cancer Res.* **65**:605–612 (2005).
107. C. A. Cuenod, L. Fournier, D. Balvay, and J. M. Guinebretiere. Tumor angiogenesis: pathophysiology and implications for contrast-enhanced MRI and CT assessment. *Abdom. Imaging* **31**:188–193 (2006).
108. D. Hanahan and J. Folkman. Patterns and emerging mechanisms of the angiogenic switch during tumorigenesis. *Cell* **86**:353–364 (1996).
109. R. P. Hill, K. De Jaeger, A. Jang, and R. Cairns. pH, hypoxia and metastasis. *Novartis Found. Symp.* **240**:154–165 (2001).
110. P. Carmeliet and R. K. Jain. Angiogenesis in cancer and other diseases. *Nature* **407**:249–257 (2000).
111. P. Carmeliet, V. Ferreira, G. Breier, S. Pollefeyt, L. Kieckens, M. Gertsenstein, M. Fahrig, A. Vandenhoeck, K. Harpal, C. Eberhardt, C. Declercq, J. Pawling, L. Moons, D. Collen, W. Risau, and A. Nagy. Abnormal blood vessel development and lethality in embryos lacking a single VEGF allele. *Nature* **380**:435–439 (1996).
112. N. Ferrara, K. Carver-Moore, H. Chen, M. Dowd, L. Lu, K. S. O'Shea, L. Powell-Braxton, K. J. Hillan, and M. W. Moore. Heterozygous embryonic lethality induced by targeted inactivation of the VEGF gene. *Nature* **380**:439–442 (1996).
113. W. Risau and V. Lemmon. Changes in the vascular extracellular matrix during embryonic vasculogenesis and angiogenesis. *Dev. Biol.* **125**:441–450 (1988).
114. V. Goede, T. Schmidt, S. Kimmina, D. Kozian, and H. G. Augustin. Analysis of blood vessel maturation processes during cyclic ovarian angiogenesis. *Lab. Invest.* **78**:1385–1394 (1998).
115. Z. Zhou, J. Wang, R. Cao, H. Morita, R. Soininen, K. M. Chan, B. Liu, Y. Cao, and K. Tryggvason. Impaired angiogenesis, delayed wound healing and retarded tumor growth in perlecan heparan sulfate-deficient mice. *Cancer Res.* **64**:4699–4702 (2004).
116. K. A. Thomas. Vascular endothelial growth factor, a potent and selective angiogenic agent. *J. Biol. Chem.* **271**:603–606 (1996).
117. T. L. Haas and J. A. Madri. Extracellular matrix-driven matrix metalloproteinase production in endothelial cells: implications for angiogenesis. *Trends Cardiovasc. Med.* **9**:70–77 (1999).
118. J. E. Nor, J. Christensen, D. J. Mooney, and P. J. Polverini. Vascular endothelial growth factor (VEGF)-mediated angiogenesis is associated with enhanced endothelial cell survival and induction of Bcl-2 expression. *Am. J. Pathol.* **154**:375–384 (1999).
119. J. Tran, J. Rak, C. Sheehan, S. D. Saibil, E. LaCasse, R. G. Korneluk, and R. S. Kerbel. Marked induction of the IAP family antiapoptotic proteins survivin and XIAP by VEGF in vascular endothelial cells. *Biochem. Biophys. Res. Commun.* **264**:781–788 (1999).
120. A. R. Pries, B. Reglin, and T. W. Secomb. Structural response of microcirculatory networks to changes in demand: information transfer by shear stress. *Am. J. Physiol. Heart Circ. Physiol.* **284**:H2204–H2212 (2003).
121. S. Rockwell, J. Yuan, S. Peretz, and P. M. Glazer. Genomic instability in cancer. *Novartis Found. Symp.* **240**:133–142; (2001) (discussion 142–151).
122. R. J. Gillies, N. Raghunand, G. S. Karczmar, and Z. M. Bhujwalla. MRI of the tumor microenvironment. *J. Magn. Reson. Imaging* **16**:430–450 (2002).
123. N. Raghunand, R. A. Gatenby, and R. J. Gillies. Microenvironmental and cellular consequences of altered blood flow in tumours. *Br. J. Radiol.* **76**:S11–S22 (2003).
124. J. C. Lee, N. H. Chow, S. T. Wang, and S. M. Huang. Prognostic value of vascular endothelial growth factor expression in colorectal cancer patients. *Eur. J. Cancer* **36**:748–753 (2000).
125. Y. Liang, R. A. Brekken, and S. M. Hyder. Vascular endothelial growth factor induces proliferation of breast cancer cells and inhibits the anti-proliferative activity of anti-hormones. *Endocr. Relat. Cancer* **13**:905–919 (2006).
126. H. Takizawa, K. Kondo, H. Fujino, K. Kenzaki, T. Miyoshi, S. Sakiyama, and A. Tangoku. The balance of VEGF-C and

VEGFR-3 mRNA is a predictor of lymph node metastasis in non-small cell lung cancer. *Br. J. Cancer* **95**:75–79 (2006).
127. G. Soufla, S. Sifakis, S. Baritaki, A. Zafiropoulos, E. Koumantakis, and D. A. Spandidos. VEGF, FGF2, TGFB1 and TGFBR1 mRNA expression levels correlate with the malignant transformation of the uterine cervix. *Cancer Lett.* **221**:105–118 (2005).
128. N. Ferrara. VEGF as a therapeutic target in cancer. *Oncology* **69**:11–16 (2005).
129. FDA. New targeted therapy for rare stomach, kidney cancers. *FDA Consum.* **40**:5 (2006).
130. S. B. Wedam, J. A. Low, S. X. Yang, C. K. Chow, P. Choyke, D. Danforth, S. M. Hewitt, A. Berman, S. M. Steinberg, D. J. Liewehr, J. Plehn, A. Doshi, D. Thomasson, N. McCarthy, H. Koeppen, M. Sherman, J. Zujewski, K. Camphausen, H. Chen, and S. M. Swain. Antiangiogenic and antitumor effects of bevacizumab in patients with inflammatory and locally advanced breast cancer. *J. Clin. Oncol.* **24**:769–777 (2006).
131. B. Morgan, A. L. Thomas, J. Drevs, J. Hennig, M. Buchert, A. Jivan, M. A. Horsfield, K. Mross, H. A. Ball, L. Lee, W. Mietlowski, S. Fuxuis, C. Unger, K. O'Byrne, A. Henry, G. R. Cherryman, D. Laurent, M. Dugan, D. Marme, and W. P. Steward. Dynamic contrast-enhanced magnetic resonance imaging as a biomarker for the pharmacological response of PTK787/ZK 222584, an inhibitor of the vascular endothelial growth factor receptor tyrosine kinases, in patients with advanced colorectal cancer and liver metastases: results from two phase I studies. *J. Clin. Oncol.* **21**:3955–3964 (2003).
132. M. Rudin, P. M. McSheehy, P. R. Allegrini, M. Rausch, D. Baumann, M. Becquet, K. Brecht, J. Brueggen, S. Ferretti, F. Schaeffer, C. Schnell, and J. Wood. PTK787/ZK222584, a tyrosine kinase inhibitor of vascular endothelial growth factor receptor, reduces uptake of the contrast agent GdDOTA by murine orthotopic B16/BL6 melanoma tumours and inhibits their growth *in vivo*. *NMR Biomed.* **18**:308–321 (2005).
133. G. Liu, H. S. Rugo, G. Wilding, T. M. McShane, J. L. Evelhoch, C. Ng, E. Jackson, F. Kelcz, B. M. Yeh, F. T. Lee Jr., C. Charnsangavej, J. W. Park, E. A. Ashton, H. M. Steinfeldt, Y. K. Pithavala, S. D. Reich, and R. S. Herbst. Dynamic contrast-enhanced magnetic resonance imaging as a pharmacodynamic measure of response after acute dosing of AG-013736, an oral angiogenesis inhibitor, in patients with advanced solid tumors: results from a phase I study. *J. Clin. Oncol.* **23**:5464–5473 (2005).
134. K. L. Li, L. J. Wilmes, R. G. Henry, M. G. Pallavicini, J. W. Park, D. D. Hu-Lowe, T. M. McShane, D. R. Shalinsky, Y. J. Fu, R. C. Brasch, and N. M. Hylton. Heterogeneity in the angiogenic response of a BT474 human breast cancer to a novel vascular endothelial growth factor-receptor tyrosine kinase inhibitor: assessment by voxel analysis of dynamic contrast-enhanced MRI. *J. Magn. Reson. Imaging* **22**:511–519 (2005).
135. P. Marzola, A. Degrassi, L. Calderan, P. Farace, E. Nicolato, C. Crescimanno, M. Sandri, A. Giusti, E. Pesenti, A. Terron, A. Sbarbati, and F. Osculati. Early antiangiogenic activity of SU11248 evaluated *in vivo* by dynamic contrast-enhanced magnetic resonance imaging in an experimental model of colon carcinoma. *Clin. Cancer Res.* **11**:5827–5832 (2005).
136. B. Giantonio, D. Levy, P. O'Dwyer, N. Meropol, P. Catalano, and A. Benson 3rd. A phase II study of high-dose bevacizumab in combination with irinotecan, 5-fluorouracil, leucovorin, as initial therapy for advanced colorectal cancer: results from the eastern cooperative oncology group study E2200. *Ann. Oncol.* **17**:1399–1403 (2006).
137. H. I. Hurwitz, L. Fehrenbacher, J. D. Hainsworth, W. Heim, J. Berlin, E. Holmgren, J. Hambleton, W. F. Novotny, and F. Kabbinavar. Bevacizumab in combination with fluorouracil and leucovorin: an active regimen for first-line metastatic colorectal cancer. *J. Clin. Oncol.* **23**:3502–3508 (2005).
138. A. Preda, V. Novikov, M. Moglich, K. Turetschek, D. M. Shames, R. C. Brasch, F. M. Cavagna, and T. P. Roberts. MRI monitoring of Avastin antiangiogenesis therapy using B22956/1, a new blood pool contrast agent, in an experimental model of human cancer. *J. Magn. Reson. Imaging* **20**:865–873 (2004).
139. W. B. Pope, A. Lai, P. Nghiemphu, P. Mischel, and T. F. Cloughesy. MRI in patients with high-grade gliomas treated with bevacizumab and chemotherapy. *Neurology* **66**:1258–1260 (2006).
140. R. R. Jennens, M. A. Rosenthal, G. J. Lindeman, and M. Michael. Complete radiological and metabolic response of metastatic renal cell carcinoma to SU5416 (semaxanib) in a patient with probable von Hippel-Lindau syndrome. *Urol. Oncol.* **22**:193–196 (2004).